coatings

MDPI

Article

Formation of Chitosan/Sodium Phytate/Nano-Fe_3O_4 Magnetic Coatings on Wood Surfaces via Layer-by-Layer Self-Assembly

Tingli Tang and Yanchun Fu *

College of Furnishings and Industrial Design, Nanjing Forestry University, Nanjing 210037, China; tangtingli777@163.com

* Correspondence: yanchunfu@njfu.edu.cn; Tel.: +86-25-8542-7793

Received: 7 December 2019; Accepted: 3 January 2020; Published: 6 January 2020

Abstract: Magnetic wood would have potential uses in electromagnetic shielding and electromagnetic wave absorption. In this paper, magnetic coatings on a wood surface were synthesized using a layer-by-layer self-assembly method. As the cationic polyelectrolyte carrier, natural macromolecular chitosan was pre-immobilized on a wood surface first, followed by the alternate adsorption of anionic polyelectrolyte sodium phytate and positively-charged Fe_3O_4 nanoparticles. The concentration of pH-controlled chitosan solution, sodium phytate solution, and Fe_3O_4 nanoparticle suspension, soaking time, and the number of alternating sedimentary layers varied. The morphology and crystal structure of the Fe_3O_4 modified wood samples were studied using scanning electron microscopy (SEM) and X-ray diffraction (XRD). The magnetic hysteresis loops showed that the modified wood had magnetic properties which were improved as the number of assembled layers increased.

Keywords: wood; magnetic; Fe_3O_4 nanoparticles; natural macromolecular polyelectrolyte; layer-by-layer self-assembly

1. Introduction

Magnetic wood is a novel biomass composite material with magnetic characteristics that retains its original wood texture, high strength-to-weight ratio, low density, easy processing, and molding [1–3]. It also has other special properties due to the addition of magnetic materials, including magnetic attraction and wave absorption, which allow it to be used for indoor electromagnetic wave absorption, heating plates, and heavy metal absorption. Such materials have promising application prospects in electromagnetic shielding and other fields [4–6].

There are currently several typical ways to prepare magnetic wood. The Oka group first proposed magnetic wood, which was obtained by combining wood with a magnetic fluid or powder loading and coating [7–9]. The Chanana group used native biomaterial wood with intrinsic anisotropy and hierarchy as a directional scaffold for the incorporation of magnetic nanoparticles inside the wood. Nanocrystalline iron oxide particles were synthesized via the in situ coprecipitation of ferric and ferrous ions within an interconnected pore network of bulk wood [10]. Segmehl et al. prepared a magnetic hybrid material derived from wood and superparamagnetic iron oxide nanoparticles (SPIONs) using microwave-assisted thermal decomposition. This novel in situ functionalization approach resulted in a homogeneous distribution of the integrated inorganic component throughout the entire complex wood cell wall structure [11]. Gan et al. prepared magnetic wood composites by modification with magnetic $CoFe_2O_4$ and hydroxyapatite (HAP) via a hydrothermal process and improved thermal stability and mechanical properties as well as UV resistance [12]. Sun et al. successfully prepared a magnetic microencapsulated phase-change energy storage wood composite using a sol-gel method,

in which microcapsules containing n-eicosane as the core and Fe_3O_4/SiO_2 as the shell were adhered to the wood surface [13].

In recent years, self-assembly techniques based on polyelectrolytes which are oppositely-charged from matrix surfaces have seen increasing applications in wood science. By non-covalently attaching a water-soluble polyelectrolyte, a controllable functional film layer can be created on the surface of wood fibers at room temperature without the aid of complex instruments and equipment [14–16]. Wood surface is rich in hydroxyl groups which are electronegative in aqueous solution and can be used to assemble polycation layers, which are the basis for subsequent polyanionic layers and nanoparticles. Renneckar et al. and Rao et al. both demonstrated that wood surface modification by attaching polyelectrolytes in a layer-by-layer assembly method provided a path to creating functional surfaces in a controlled manner [17,18].

In addition to traditional polyelectrolytes such as polyacrylamine hydrochloride, sodium polystyrene sulfonate, etc., natural macromolecules such as chitosan, pectin, alginate, and xanthan gum, etc. are also ideal materials for layer-by-layer assembly [19–21]. Compared with synthetic polyelectrolytes with high crystallinities and low melting points, which lead to narrow processing temperature ranges, low permeability, and poor interface stability, natural polyelectrolytes are highly water-soluble and have excellent adsorption abilities and interfacial stabilities [22–24]. For example, dopamine is a self-adhesive "biological glue" that firmly adheres many polymers to the surface of basement membranes [25].

In this work, a natural macromolecular-based coating with adjoined magnetic Fe_3O_4 nanoparticles was designed for wood surface modification. Chitosan was first immobilized on a wood surface in an interfacial layer, and then multilayer coatings were obtained by alternating layer-by-layer deposition of sodium phytate and Fe_3O_4 nanoparticles. The magnetic activity of the coatings was also tested. Through process is in an early development stage, it provides a more efficient combination scheme and provides a theoretical basis and technical guidance for a practical wood modification method.

2. Materials and Methods

2.1. Materials

Balsa wood blocks (purchased from Suzhou Zhonglin Wansen Wood Industry Co., Ltd., Suzhou, China) were formed into 10 mm (Longitudinal) × 10 mm (Tangential) × 10 mm (Radial) small wood blocks. Chitosan (low viscosity: <200 mPa.s), sodium phytate (99.0% metals basis), and Fe_3O_4 nanoparticles (99.0% metals basis, 20 nm) used to prepare magnetic coatings were purchased from Shanghai Aladdin Bio-Chem Technology Co., Ltd., Shanghai, China. Hydrochloric acid (36.5–38.0%, BioReagent, for molecular biology) was purchased from Sigma-Aldrich (Shanghai, China), and deionized water was provided by Barnstead Nanopure Diamond Laboratory water system (Gilroy, CA, USA). Wood specimens were immersed in a beaker filled with distilled water to clean and remove dust and grease from the wood surface. They were then placed into an oven set to 60 °C and dried for 2 h.

2.2. Preparation of Cationic and Anionic Polyelectrolyte Solutions

Cationic polyelectrolyte solutions were prepared by first dissolving 0.5, 1, or 2 g chitosan powder in 100 mL distilled water with a constant stirring speed. The pH of all solutions was adjusted to 2.5 with dilute hydrochloric acid, which protonated the amino group of chitosan and resulted in a positively-charged solution.

In the same manner, anionic polyelectrolyte solutions were prepared by dissolving 0.5, 1, or 2 g sodium phytate powder in 100 mL distilled water with a constant stirring speed. The pH of all solutions was adjusted to 2.5 with dilute hydrochloric acid. Since sodium phytate is a natural polyanion, the obtained solutions were negatively-charged.

2.3. Preparation of Positively-Charged Fe_3O_4 Nanoparticles Suspension

Positively-charged Fe_3O_4 nanoparticle suspension were prepared by first dissolving 0.5, 1, or 2 g Fe_3O_4 nanoparticles powder in 100 mL distilled water at a constant stirring speed. The pH of all solutions was adjusted to 2.5 with dilute hydrochloric acid. Fe_3O_4 is a common metal oxide with an isoelectric point between 6.5 and 6.8 [26]. Since the pH of the prepared solutions was lower than the isoelectric point of Fe_3O_4, they were positively-charged.

2.4. Formation of Magnetic Coatings on Wood Surfaces by Layer-by-Layer Self-Assembly

First, wood samples were pre-treated by immersion in a chitosan cationic polyelectrolyte solution. Since the wood surface was negatively-charged in the aqueous solution, the polycationic assembled on the wood surface via electrostatic adsorption. After a certain period of time, the wood sample was removed and washed with distilled water and then placed in an oven at 60 °C for 1 h. Then, the chitosan-wood was immersed in a sodium phytate anionic polyelectrolyte solution. At this time, the chitosan-wood sample was positively-charged, which allowed the polyanion to assemble via electrostatic adsorption. After a certain period of time, the wood sample was removed and washed with distilled water and then placed in an oven at 60 °C for 1 h. Finally, the sodium phytate-chitosan-wood sample was immersed in the prepared positively-charged Fe_3O_4 nanoparticle suspension. After a certain period of time, the wood sample was removed and washed with distilled water and then placed in an oven at 60 °C for 1 h. Due to electrostatic adsorption, a Fe_3O_4 nanoparticle coating was assembled on the surface of sodium phytate-chitosan-wood. The sodium phytate anionic polyelectrolyte and the positively-charged Fe_3O_4 nanoparticles were used as the assembly units, which were alternately deposited on the wood surface until the targeted number of coating layers was achieved (Figure 1). In order to determine the optimal coating preparation conditions, the solution concentration, soaking time, and the number of alternating sedimentary layers were varied during the growth control experiment, and the original wood was used as a control.

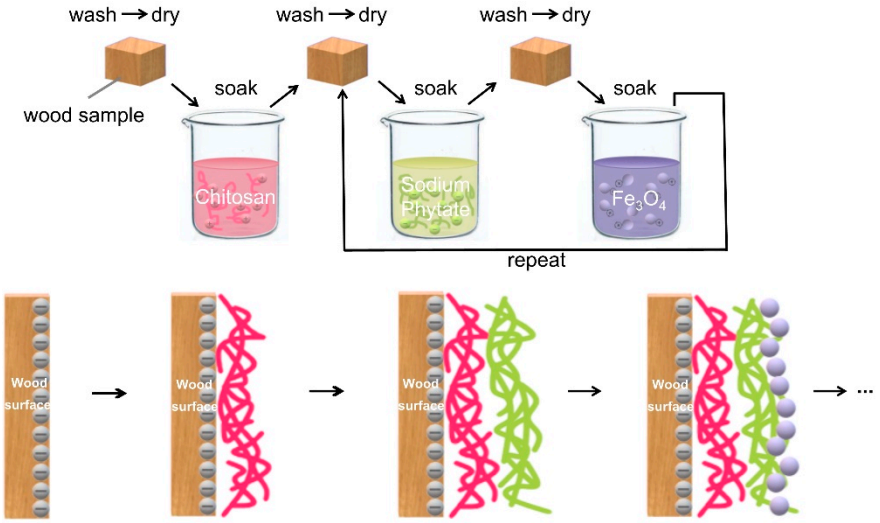

Figure 1. Scheme of fabricating magnetic coating on wood surface by layer-by-layer self-assembly.

2.5. Characterization and Analysis

The crystalline phase of the Fe_3O_4 nanoparticles on the wood surface was revealed via X-ray diffraction (XRD) using a D/MAX 2200 diffractometer (Rigaku Inc., Tokyo, Japan). The specific test parameters were a Cu target Kα radiation measured from 10°–90° at a scan rate (2θ) of 4°·min^{-1}, an accelerating voltage of 40 kV, and current of 30 mA. The surface morphology of the as-prepared samples was characterized via scanning electron microscopy (SEM), using a Quanta 400 FEG (FEI Inc.,

Eindhoven, The Netherlands) at a 20 kV operating voltage. Samples were coated with a 5–10 nm Au layer before SEM imaging.

For magnetic characterization, wood samples were cut into small sizes of 2 mm (Longitudinal × 2 mm (Tangential) × 2 mm (Radial) and measured by a vibrating sample magnetometer (VSM, PPMS-9T, Quantum Design Corp, San Diego, CA, USA) at room temperature.

3. Results and Discussion

Chitosan/sodium phytate/nano-Fe_3O_4 composite coatings on wood surfaces obtained by stepwise assembly were observed by SEM. Figure 2a shows the top view morphology of the original wood, in which differentiated microstructural details can be clearly observed. The deposition of chitosan and sodium phytate polyelectrolyte coatings gradually obscured the ultrastructural features of the cell walls, which eventually appeared smooth and masked the surface topography (Figure 2b,c). After assembly of the nano-Fe_3O_4 layer, high-magnification SEM images (Figure 2d) revealed that the Fe_3O_4 nanoparticles were densely distributed over the entire wood surface.

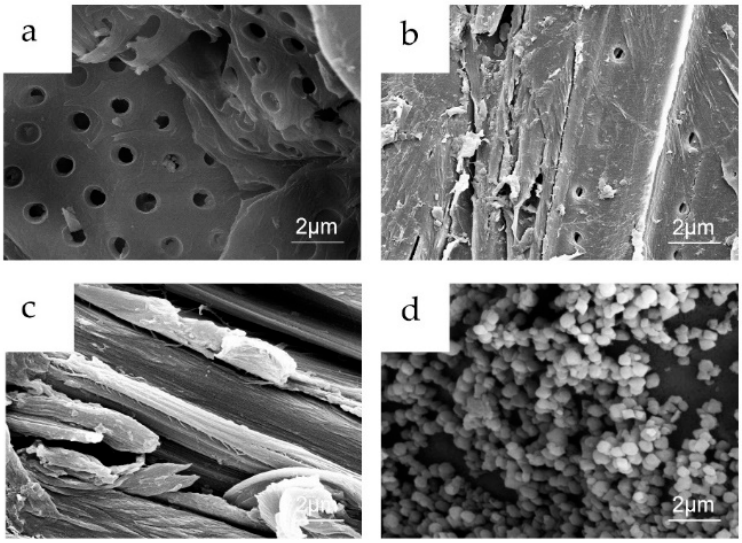

Figure 2. Scanning electron microscopy (SEM) images of chitosan/sodium phytate/nano-Fe_3O_4 composite coatings on wood surfaces obtained by stepwise assembly: (**a**) original wood, (**b**) chitosan-coated wood, (**c**) sodium phytate-chitosan-coated wood and (**d**) nano-Fe_3O_4-sodium phytate-chitosan-coated wood.

XRD patterns of the original wood and the modified wood covered with coatings using different solution concentrations are shown in Figure 3a. All wood samples showed the typical peaks of cellulose I at 2θ = 16.5° and 22.6°. Compared with the original wood, the absorption peaks of cellulose in the modified wood samples were nearly unchanged, implying that the wood composition was minimally damaged by this mild modification method. Wood samples modified using solutions (concentrations of 0.5%, 1%, and 2%) with a molar ratio of chitosan sodium phytate, and Fe_3O_4 nanoparticles of 1:1:1 clearly displayed distinct crystallographic phases in their XRD patterns. The appearance of diffraction peaks at 2θ = 35°, 43°, 58°, and 69° agrees well with the Fe_3O_4 powder standard (JCPDS 19–0629). The peak intensities notably increased with the solution concentration, probably due to the increased number of Fe_3O_4 nanoparticles.

The morphology of Fe_3O_4 particles showed some variation with the solution concentration. At lower solution concentrations, there was an insufficient number of Fe_3O_4 particles to cover the pits in wood cell walls, resulting in an uneven particle distribution (Figure 3b). At higher solution concentrations, more Fe_3O_4 particles adsorbed on the wood surface, and the film layer was gradually flattened (Figure 3c). This tendency continued until reaching a 2% solution concentration, which further

increased the amount of Fe_3O_4 particles and increased the thickness of the composite coatings; however, a certain degree of agglomeration was also observed (Figure 3d).

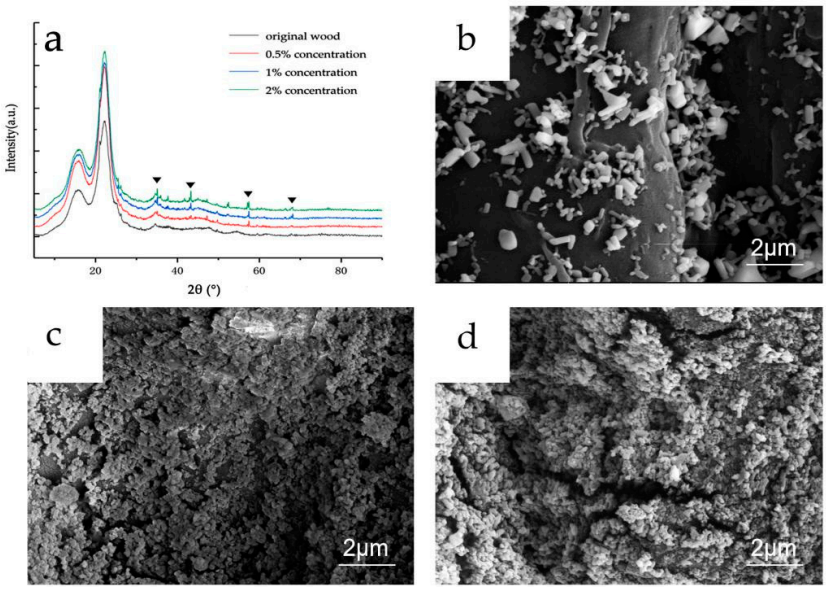

Figure 3. (**a**) X-ray diffraction (XRD) patterns of the original wood (black), concentrations of 0.5% (red), concentrations of 1% (blue), and concentrations of 2% (green); high-magnification SEM images of chitosan/sodium phytate/nano-Fe_3O_4 composite coatings on wood surfaces obtained by different solution concentrations: (**b**) 0.5%, (**c**) 1%, and (**d**) 2%.

The XRD patterns of modified wood samples obtained using 1% chitosan solution, sodium phytate solution, and Fe_3O_4 nanoparticles suspension in a molar ratio of 1:1:1 and various soaking times (30, 60, and 90 min) displayed diffraction peaks at 2θ = 35°, 43°, 58°, and 69°. The peak intensities increased with the soaking time (Figure 4a), suggesting that the soaking time greatly influenced the distribution of Fe_3O_4 nanoparticles in the final composite membrane. According to the SEM images, more Fe_3O_4 nanoparticles were adsorbed on the wood surface at longer soaking time (Figure 4b–d), which implied that the electrostatic adsorption of cations (chitosan and Fe_3O_4 nanoparticles) and anions (sodium phytate) from the solution required a certain amount of time, which was improved at longer immersion time.

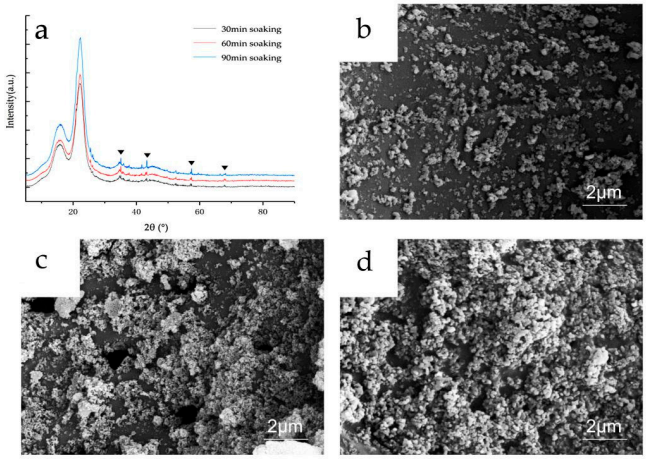

Figure 4. (**a**) XRD patterns of different soaking time: 30 (black), 60 (red), and 90 min (blue); high-magnification SEM images of chitosan/sodium phytate/nano-Fe_3O_4 composite coatings on wood surfaces obtained by different soaking time: (**b**) 30 min, (**c**) 60 min, and (**d**) 90 min.

The XRD patterns of modified wood samples with multiple layers (1, 5, and 10 bilayers) obtained from alternating sedimentary of sodium phytate and Fe_3O_4 nanoparticles contained diffraction peaks at $2\theta = 35°$, 43°, 58°, and 69°. A detailed list of the amount of materials for coatings prepared is shown in Table 1. The peak intensities increased with the number of alternating sedimentary layers added (Figure 5a). Different Fe_3O_4 nanoparticle distributions were clearly observed in the SEM images on modified chitosan-wood samples coated with different numbers of sodium phytate/nano-Fe_3O_4 bilayers (Figure 5b–d). The coating surface containing sodium phytate/nano-Fe_3O_4 1 bilayer was composed of only a few Fe_3O_4 nanoparticles. Along with increasing the number of sodium phytate/nano-Fe_3O_4 bilayers, the amount of Fe_3O_4 particles further increased, resulting in a thicker composite coating. At the same time, mass agglomeration was also observed.

Table 1. Reaction factors of the modified wood samples with multiple layers.

Layer Number	Chitosan Concentration	Sodium Phytate Concentration	Fe_3O_4 Nanoparticles Concentration	Soaking Time
1 bilayer	1%	1%	1%	90 min
5 bilayers	1%	1%	1%	90 min
10 bilayers	1%	1%	1%	90 min

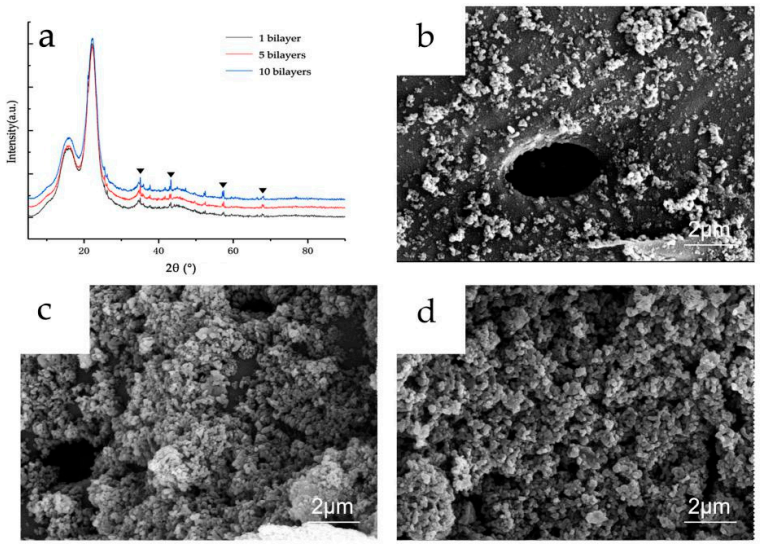

Figure 5. (**a**) XRD patterns of different numbers of alternating sedimentary layers at room temperature: 1 (black), 5 (red), and 10 bilayers (blue); high-magnification SEM images of chitosan/sodium phytate/nano-Fe_3O_4 composite coatings on wood surfaces obtained by different numbers of alternating sedimentary layers at room temperature: (**b**) 1 bilayer, (**c**) 5 bilayers, and (**d**) 10 bilayers.

The magnetic properties of wood samples coated with chitosan/sodium phytate/nano-Fe_3O_4 were measured by vibrating sample magnetometer (VSM). Figure 6 shows the magnetization curves of magnetic wood samples obtained from different numbers of alternating sedimentary layers at room temperature. All magnetic wood samples showed typical paramagnetic behavior because their magnetic hysteresis loops were very narrow and long. The magnetization saturation values (Ms) of sodium phytate/nano-Fe_3O_4 1, 5, and 10 bilayers on chitosan-wood revealed that more assembled layers of Fe_3O_4 nanoparticles on the wood surface improved the magnetic properties. The saturation magnetization of magnetic wood was lower than that of pure Fe_3O_4 nanoparticles [27], likely due to the presence of the nonmagnetic wood substrate.

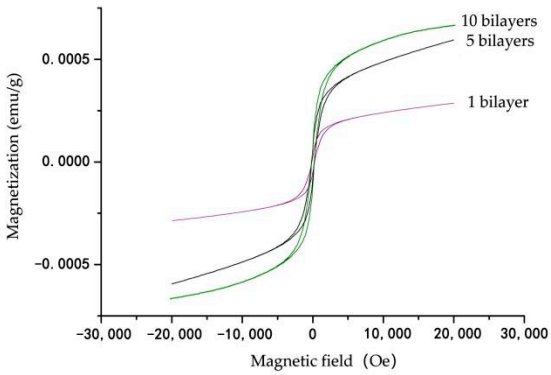

Figure 6. Vibrating sample magnetometer (VSM) curves of the magnetic wood with the number of alternating sedimentary layers at room temperature of 1 (purple), 5 (black), and 10 bilayers (green).

4. Conclusions

It was demonstrated that creating multilayered coatings on wood surfaces using Fe_3O_4 nanoparticles could be accomplished using a layer-by-layer self-assembly technique using natural macromolecular chitosan and sodium phytate as cationic and anionic polyelectrolytes. The concentration of the polyelectrolyte solution and Fe_3O_4 nanoparticles suspension, soaking time of each wood sample, and the number of alternating sedimentary layers of sodium phytate and Fe_3O_4 nanoparticles were positively correlated with the quantity and distribution of Fe_3O_4 nanoparticles in the final prepared coatings. The magnetic hysteresis loops demonstrated the paramagnetic behavior of the modified wood, whose magnetic properties increased with higher numbers of alternating sedimentary bilayers of sodium phytate and Fe_3O_4 nanoparticles on the wood surface.

Author Contributions: Conceptualization, methodology, Y.F.; software, validation, formal analysis, investigation, resources, data curation, T.T. and Y.F.; writing—original draft preparation, T.T.; writing—review and editing, Y.F. All authors have read and agreed to the published version of the manuscript.

Funding: This research was funded by Youth Science and Technology Innovation Fund of Nanjing Forestry University, grant number CX2016016.

Conflicts of Interest: The authors declare no conflict of interest.

References

1. Oka, H.; Narita, K.; Osada, H.; Seki, K. Experimental results on indoor electromagnetic wave absorber using magnetic wood. *J. Appl. Phys.* **2002**, *91*, 7008–7010. [CrossRef]
2. Oka, H.; Tanaka, K.; Osada, H.; Kubota, K. Study of electromagnetic wave absorption characteristics and component parameters of laminated-type magnetic wood with stainless steel and ferrite powder for use as building materials. *J. Appl. Phys.* **2009**, *105*, 07E701. [CrossRef]
3. Oka, H.; Terui, M.; Osada, H.; Sekino, N. Electromagnetic wave absorption characteristics adjustment method of recycled powder-type magnetic wood for use as a building material. *IEEE Trans. Magn.* **2012**, *48*, 3498–3500. [CrossRef]
4. Gan, W.T.; Liu, Y.; Gao, L.K.; Zhan, X.X.; Li, J. Magnetic property, thermal stability, UV-resistance, and moisture absorption behavior of magnetic wood composites. *Polym. Compos.* **2015**, *38*, 1646–1654. [CrossRef]
5. Gan, W.T.; Gao, L.K.; Sun, Q.F.; Jin, C.D.; Lu, Y.; Li, J. Multifunctional wood materials with magnetic, superhydrophobicand anti-ultraviolet properties. *Appl. Surf. Sci.* **2015**, *332*, 565–572. [CrossRef]
6. Gan, W.T.; Xiao, S.L.; Gao, L.K.; Gao, R.N.; Li, J.; Zhan, X.X. Luminescent and transparent wood composites fabricated by poly(methyl methacrylate) and γ-Fe_2O_3@YVO_4:Eu^{3+} nanoparticle impregnation. *ACS Sustain. Chem. Eng.* **2017**, *5*, 3855–3862. [CrossRef]
7. Oka, H.; Hojo, A.; Osada, H.; Namizaki, Y.; Taniuchi, H. Manufacturing methods and magnetic characteristics of magnetic wood. *J. Magn. Magn. Mater.* **2004**, *272–276*, 2332–2334. [CrossRef]

8. Oka, H.; Kataoka, Y.; Osada, H.; Aruga, Y.; Izumida, F. Experimental study on electromagnetic wave absorbing control of coating-type magnetic wood using a grooving process. *J. Magn. Magn. Mater.* **2007**, *310*, 1028–1029. [CrossRef]
9. Oka, H.; Uchidata, S.; Sekino, N.; Namizaki, Y.; Taniuchi, H. Electromagnetic wave absorption characteristics of half carbonized powder-type magnetic wood. *IEEE Trans. Magn.* **2011**, *47*, 3078–3080. [CrossRef]
10. Merk, V.; Chanana, M.; Gierlinger, N.; Hirt, A.M.; Burgert, I. Hybrid wood materials with magnetic anisotropy dictated by the hierarchical cell structure. *ACS Appl. Mater. Interfaces* **2014**, *6*, 9760–9767. [CrossRef]
11. Segmehl, J.S.; Laromaine, A.; Keplinger, T.; Masnou, A.M.; Roig, A. Magnetic wood by in situ synthesis of iron oxide nanoparticles via a microwave-assisted route. *J. Mater. Chem. C* **2018**, *6*, 3395–3402. [CrossRef]
12. Gan, W.T.; Gao, L.K.; Zhan, X.X.; Li, J. Hydrothermal synthesis of magnetic wood composites and improved wood properties by precipitation with $CoFe_2O_4$/hydroxyapatite. *RSC Adv.* **2015**, *5*, 45919–45927. [CrossRef]
13. Qian, T.M.; Dang, B.K.; Chen, Y.P.; Jin, C.D.; Qian, J.; Sun, Q.F. Fabrication of magnetic phase change n-eicosane@Fe_3O_4/SiO_2 microcapsules on wood surface via sol-gel method. *J. Alloys Compd.* **2019**, *772*, 871–876. [CrossRef]
14. Agarwal, M.; Lvov, Y.; Varahramyan, K. Conductive wood microfibres for smart paper through layer-by-layer nanocoating. *Nanotechnology* **2006**, *17*, 5319–5325. [CrossRef]
15. Zhao, Z.Y.; Sun, S.J.; Wu, D.; Zhang, M.; Huang, C.X.; Umemura, K.; Yong, Q. Synthesis and characterization of sucrose and ammonium dihydrogen phosphate (SADP) adhesive for plywood. *Polymers* **2019**, *11*, 1909. [CrossRef] [PubMed]
16. Koklukaya, O.; Carosio, F.; Grunlan, J.C.; Wågberg, L. Flame-retardant paper from wood fibers functionalized via layer by-layer assembly. *ACS Appl. Mater. Interfaces* **2015**, *7*, 23750–23759. [CrossRef]
17. Renneckar, S.; Zhou, Y. Nanoscale coatings on wood: Polyelectrolyte adsorption and layer-by-layer assembled film formation. *ACS Appl. Mater. Interfaces* **2009**, *1*, 559–566. [CrossRef]
18. Rao, X.; Liu, Y.Z.; Fu, Y.C.; Liu, Y.X.; Yu, H.P. Formation and properties of polyelectrolytes/TiO_2 composite coating on wood surfaces through layer-by-layer assembly method. *Holzforschung* **2016**, *70*, 361–367. [CrossRef]
19. Decher, G.; Hong, J.D. Buildup of ultrathin multilayer films by a self-assembly process, 1 consecutive adsorption of anionic and cationic bipolar amphiphiles on charged surfaces. *Macromol. Symp.* **1991**, *46*, 321–327. [CrossRef]
20. Schoeler, B.; Guruswamy, K.A.; Caruso, F. Investigation of the influence of polyelectrolyte charge density on the growth of multilayer thin films prepared by the layer-by-layer technique. *Macromolecules* **2002**, *35*, 889–897. [CrossRef]
21. Bieker, P.; Schönhoff, M. Linear and exponential growth regimes of multilayers of weak polyelectrolytes in dependence on pH. *Macromolecules* **2010**, *43*, 5052–5059. [CrossRef]
22. Li, Q.; Du, Y.Z.; Yuan, H.; Zhang, X.G.; Miao, J.; Cui, F.D.; Hu, F.Q. Synthesis of lamivudine stearate and antiviral activity of stearic acid-g-chitosan oligosaccharide polymeric micelles delivery system. *Eur. J. Pharm. Sci.* **2010**, *41*, 498–507. [CrossRef] [PubMed]
23. Sadeghi-Kiakhani, M.; Arami, M.; Gharanjig, K. Preparation of chitosan-ethyl acrylate as a biopolymer adsorbent for basic dyes removal from colored solutions. *J. Environ. Chem. Eng.* **2013**, *1*, 406–415. [CrossRef]
24. Kai, C.; Catchmark, J.M. Improved eco-friendly barrier materials based on crystalline nanocellulose/chitosan/carboxymethyl cellulose polyelectrolyte complexes. *Food Hydrocoll.* **2018**, *80*, 195–205.
25. Shi, H.Y.; Xue, L.X.; Gao, A.L.; Fu, Y.Y.; Zhou, Q.B.; Zhu, L.J. Fouling-resistant and adhesion-resistant surface modification of dual layer PVDF hollow fiber membrane by dopamine and quaternary polyethyleneimine. *J. Membr. Sci.* **2016**, *498*, 39–47. [CrossRef]
26. Chen, M.J.; Shen, H.; Li, X.; Liu, H.F. Facile synthesis of oil-soluble Fe_3O_4 nanoparticles based on a phase transfer mechanism. *Appl. Surf. Sci.* **2014**, *307*, 306–310. [CrossRef]
27. Gan, W.T.; Gao, L.K.; Xiao, S.L.; Gao, R.N.; Li, J.; Zhan, X.X. Magnetic wood as an effective induction heating material: Magnetocaloric effect and thermal insulation. *Adv. Mater. Interfaces* **2017**, *4*, 1700777. [CrossRef]